

## Article

# Influence of Wetting Conditions and Concrete Strength of Both Substrate and Repair Material on the Bond Capacity of Repaired Joints

Vinicius Brother dos Santos , Ana Paula Pereira dos Santos Silva , Bernardo Lopes Poncetti ,  
Lucas Dezotti Tolentino , Pablo Augusto Krahl  and Romel Dias Vanderlei 

Department of Civil Engineering, State University of Maringá, Av. Colombo n° 5790,  
Maringá 87020-900, PR, Brazil

\* Correspondence: brothervinicius@gmail.com

**Abstract:** Ultra-high performance concrete (UHPC) is an appropriate material to repair and rehabilitate aged structures due to its excellent properties, such as high compressive strength and durability. Several studies have demonstrated the effectiveness of applying UHPC in old buildings as a rehabilitation or repair material, but the bond between concretes needs more investigation. In this sense, the bond between normal-strength concrete (NSC) and UHPC is currently being studied. Three main parameters are responsible for ensuring a good bond: the surface treatment of the substrate (roughness), the wetting conditions, and the mechanical strength of the substrate. Thus, the present study investigated the bond between concretes experimentally. The concrete of the substrate was carried out in three grades: C25, C45, and C60. The repair concretes were C25, C45, C60, and UHPC. The following parameters were evaluated: wetting conditions, air surface dry (ASD), saturated surface dry (SSD), substrate strength, and repair concrete strength. All models received surface treatment by wire brushing. Slant shear and splitting tensile tests were performed to evaluate the mechanical behavior and the failure modes of the bond between concretes. The bond strength was classified and compared to existing predicting models. The results showed that most expressive strength gains occurred in SSD models with lower strength substrates and UHPC. Furthermore, the influence of surface wetting conditions becomes smaller as the strength of the substrate is reduced.

**Keywords:** ultra-high performance concrete (UHPC); high-strength concrete (HSC); normal strength concrete (NSC); slant shear test; splitting tensile test; bond strength; friction coefficient



**Citation:** Santos, V.B.d.; Santos Silva, A.P.P.d.; Poncetti, B.L.; Tolentino, L.D.; Krahl, P.A.; Vanderlei, R.D. Influence of Wetting Conditions and Concrete Strength of Both Substrate and Repair Material on the Bond Capacity of Repaired Joints. *Buildings* **2023**, *13*, 643. <https://doi.org/10.3390/buildings13030643>

Academic Editors: Junjie Zeng and Roberto Capozucca

Received: 18 January 2023

Revised: 8 February 2023

Accepted: 24 February 2023

Published: 28 February 2023



**Copyright:** © 2023 by the authors. Licensee MDPI, Basel, Switzerland. This article is an open access article distributed under the terms and conditions of the Creative Commons Attribution (CC BY) license (<https://creativecommons.org/licenses/by/4.0/>).

## 1. Introduction

Globally, many existing concrete structures need effective and durable repairs. Most structures were made by normal or high-strength concretes exposed to weathering actions and chemical attacks. Ultra-high performance concrete (UHPC) is a material that could potentially be used for the rehabilitation or repair of structures [1–9]. The successful application of UHPC as a structural rehabilitation material is attributed to its properties, e.g., high compressive strength, high tenacity, and very low permeability to external agents [10]. On the other hand, some aspects must be considered when specifying the material and adequate thickness for repairing structures, such as its behavior by exposure to elevated temperatures and the adequate structural response [11]. Furthermore, the UHPC can replace other concretes in some applications in shear key joints in bridge engineering or shear pockets of composite steel–UHPC structures [12,13]. However, the bond between the repair material and substrate must be adequately defined to guarantee the adequate performance of the retrofit [14–18]. Thus, it is essential to evaluate the behavior of the bond between different concrete grades with some wetting conditions of the substrate. Furthermore, it is necessary to evaluate prediction models for the bond between concretes.

The research was carried out to investigate the NSC–UHPC bond. Harris, Sarkar, and Ahlborn [19] performed slant shear and splitting tensile tests to investigate the NSC–UHPC bond. Four methods for the substrate surface treatment were proposed: smooth (as cast), chipped, grooved, and shear keys. Smooth samples failed at the interface, while specimens with low roughness (chipped), grooved, and shear keys failed at the substrate. The results indicated that the bond strength could exceed the substrate strength with proper surface treatment. When observing the minimum bonding performance requirements from the ACI 546.3R-14 [20] and Sprinkel and Ozyildirim [21] guides, the authors concluded that UHPC provides good bonding for various surface treatments. Ahallaq, Tayeh, and Shihada found a similar conclusion in their study [17]. Tayeh et al. [10,22] studied the NSC–UHPC bond with five different substrate surface treatments: smooth (as cast), sandblasted, wire brushed, drilled holes, and grooved. The sandblasted surface demonstrated the best results in the splitting tensile test and was the only one to generate results that met the requirements of the ACI 546.3R-14 [20] for the slant shear tests. Other research studies confirm the efficiency of the sandblasting method for the NSC–UHPC adherence [23–25]. Carbonell Muñoz et al. [4] adopted the roughness of the substrate as smooth (as cast), chipped, wire brushed, sandblasted, and grooved, and evaluated two wetting conditions of the concrete substrate—dry and saturated. The results showed that the performance of the NSC–UHPC bond is suitable, regardless of the degree of roughness of the substrate, except when the substrate had a dry wetting condition. The authors concluded that a simple treatment that removes dust and debris from the substrate might be sufficient to obtain an excellent NSC–UHPC bond, provided it has the correct wetting conditions. Farzad, Shafieifar, and Azizinamini [7] experimentally and numerically analyzed the NSC–UHPC bond with the surface of the dry and wet substrate. The samples with the wet substrate showed the best results. Another analogous study by Zhang et al. [26] considered different types of surface treatments, and except for the grooved and bonded rebar treatment, all of the samples showed brittle failure. Zhang et al. [27] studied the influences of three moisture degrees of NSC substrate in different substrate treatments: air surface dry (ASD), i.e., subjecting the substrate to room temperature for more than seven days before UHPC overlay; air surface wet (ASW), i.e., spraying water on the substrate for approximately 20 min and wiping with a dry towel (before the UHPC overlay); and saturated surface dry (SSD), where the substrate was submerged in water for 24 h and then dried with compressed air before the UHPC overlay. The surface with low roughness provided the best results, and the smooth surface (without treatment) presented the worst results. Compared with the reference samples (ASD), the ASW and SSD wetting degrees provided the brushed surface samples with mean percentage increases of 34.4% and 49.0%, respectively. Zhang et al. [28] reached similar conclusions. The authors recommend that when applying UHPC as a repair material, the concrete substrate should be saturated for at least 10 h, considering the short construction time. The high porosity of the NSC substrate can transfer water through the interface, reducing the water in UHPC and generating incomplete cement hydration, which weakens the NSC–UHPC bond [27]. Recent studies proposed by Zhang et al. [27] used two grades of NSC (C30 and C40) and one grade of HSC (C60) as substrate material. The bond strength was observed to increase with the substrate strength [27]. Similar conclusions were found in the research by Zhang et al. [26,28], using two grades of NSC (C30, C40, and C50) for the substrate. However, further investigation is needed to study the influence of wetting conditions and other concrete grades. According to AASHTO LRFD [29], the friction coefficient of the NSC–UHPC bond can be calculated through the cohesion results obtained from the direct tensile tests, as well as the results from the slant shear tests. However, other studies show that cohesion is equal to the results of splitting tensile tests [15,30–32].

The main objective of the present study was to investigate the bond between different grades of concrete through slant shear and splitting tensile tests. The substrate concrete was tested in three grades: C25, C45, and C60, while the repair concretes were of the same substrate classes (C25, C45, and C60) or UHPC. In addition, monolithic models were

produced for comparison purposes. The parameters evaluated were the wetting conditions of the substrate, the strength of the substrate, and the strength of the repair material. The substrate surface was treated by wire brushing.

## 2. Materials and Methods

### 2.1. Mix Proportion of Materials

This experimental program utilized NSC and HSC as both substrate and repair materials, while UHPC was solely used as a repair material. The NSC and HSC were produced using Portland cement type III, natural river sand with a fineness modulus of 1.519, crushed basalt stone coarse aggregates with particle sizes ranging from 4.75 to 12.5 mm, and a water reducer of either lignosulfonate or polycarboxylate, along with water. The UHPC was composed of Portland cement type III, quartz sand with particle sizes of 0.075 and 0.60 mm, having a density of 2.65 g/cm<sup>3</sup>, quartz powder containing 99.68% SiO<sub>2</sub> with particle sizes less than 0.045 mm, silica fume containing 94.1% SiO<sub>2</sub> with particle sizes from 0.02 to 0.11 mm, and a specific surface area of 24.7 m<sup>2</sup>/kg, polycarboxylate water reducer, and water. The mix proportions of concretes and UHPC are presented in Table 1.

**Table 1.** Constituent of concretes and UHPC (kg/m<sup>3</sup>).

Constituents	C25	C45	C60	UHPC
Portland cement (Type III)	302.9	418.1	502.7	769.9
Quartz sand ( $\leq 1180 \mu\text{m}$ )	852.0	764.2	766.2	–
River sand ( $F.M. = 1.519$ )	–	–	–	846.9
Coarse aggregate (max. 12.5 mm)	1109.7	1135.9	1080.9	–
Quartz powder ( $\leq 45 \mu\text{m}$ )	–	–	–	384.9
Silica fume (24.7 m <sup>2</sup> /g)	–	–	–	192.5
Water	193.8	179.8	170.9	177.1
Lignosulfonate water reducer	1.2	2.1	–	–
Polycarboxylate water reducer	–	–	1.5	23.1
w/c	0.64	0.43	0.34	0.23

The mechanical properties of concretes and UHPC were obtained through the technical standards ABNT NBR 5739 [33], ASTM C496 [34], and ABNT NBR 8522-1 [35], for the axial compressive strength, splitting tensile test, and elastic modulus tests, respectively. The specimens used were cylindrical with dimensions of  $\phi 100 \times 200$  mm for the concrete and  $\phi 50 \times 100$  mm for the UHPC. The specimens were kept in moist storage until the test date.

### 2.2. Test Specimens and Preparation

#### 2.2.1. Test Specimens

The slant shear test was performed according to the ASTM C882 technical standard [36], as illustrated in Figure 1. Prismatic specimens with a square cross-section of 100 × 100 mm and a height of 300 mm were adopted, similar to other research [10,22–24,27,37]. The bond surface between the concretes formed an angle of 30° with the longitudinal axis (direction of loading), as shown in Figure 1. The bond strength can be calculated using (1):

$$f_n = \frac{P}{A_n}, A_n = \frac{A}{\sin \alpha}, \sigma_n = f_n \sin \alpha, \tau_n = f_n \cos \alpha \quad (1)$$

where  $f_n$  is the bond strength by the slant shear (MPa);  $\sigma_n$  and  $\tau_n$  are, respectively, the normal compressive stress and shear stress acting on the inclined plane (MPa);  $P$  is the maximum load obtained in the test (N);  $A$  is the cross-sectional area (mm<sup>2</sup>);  $A_n$  is the section area on the inclined plane (mm<sup>2</sup>);  $\alpha$  is the angle between the longitudinal axis and the bonding surface (30°).

The splitting tensile test was performed following the guidelines of the ASTM C496 technical standard [34], using cylindrical specimens that were 100 mm in diameter and 200 mm in length; see Figure 1. The bond strength can be calculated from (2).

$$f_{sp} = \frac{2P}{\pi dl} \quad (2)$$

where  $f_{sp}$  is the splitting tensile strength (MPa);  $P$  is the maximum load obtained in the test (N);  $d$  is the diameter of the specimen (mm);  $l$  is the length of the specimen (mm).

For the slant shear test, the loading rate adopted was 2.50 kN/s; values were adopted from a study by Carbonell Muñoz [38] and the ASTM C39 technical standards [39]. For the splitting tensile test, the loading rate adopted was 0.45 kN/s and values were adopted from a study by Carbonell Muñoz [38] and the ASTM C496 technical standards [34].

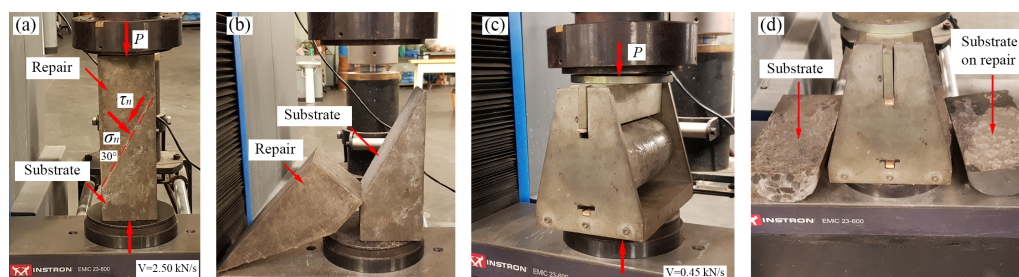


**Figure 1.** Slant shear and splitting tensile tests: (a) slant shear test; (b) bond failure; (c) splitting tensile test; (d) bond failure.

Each group is identified in the X–Y–Z format, where X is the substrate-wetting conditions, i.e., air surface dry (ASD) or saturated surface dry (SSD); Y is the substrate concrete: C25, C45, and C60; and Z is the repair concrete: C25, C45, C60, and UHPC. In addition, for comparison, monolithic models were produced, identified as C25, C45, or C60. Table 2 presents the group nomenclature of the studied specimens.

**Table 2.** Group nomenclature of studied specimens.

Specimen Number	Group Name	Description
1	C25	Monolithic model of C25 concrete
2	ASD-C25-C25	Model with bond between C25 concrete and ASD substrate
3	ASD-C25-UHPC	Model with bond between C25 concrete and UHPC with ASD substrate
4	SSD-C25-C25	Model with bond between C25 concrete and SSD substrate
5	SSD-C25-UHPC	Model with bond between C25 concrete and UHPC with SSD substrate
6	C45	Monolithic model of C45 concrete
7	ASD-C45-C45	Model with bond between C45 concrete and ASD substrate
8	ASD-C45-UHPC	Model with bond between C45 concrete and UHPC with ASD substrate
9	SSD-C45-C45	Model with bond between C45 concrete and SSD substrate
10	SSD-C45-UHPC	Model with bond between C45 concrete and UHPC with SSD substrate
11	C60	Monolithic model of C60 concrete
12	ASD-C60-C60	Model with bond between C60 concrete and ASD substrate
13	ASD-C60-UHPC	Model with bond between C60 concrete and UHPC with ASD substrate
14	SSD-C60-C60	Model with bond between C60 concrete and SSD substrate
15	SSD-C60-UHPC	Model with bond between C60 concrete and UHPC with SSD substrate

## 2.2.2. Specimen Preparation

For the monolithic models, specimens were made using C25, C45, and C60 concretes. Mechanical tests were carried out after 28 days of curing the monolithic models in moist storage. Bond investigation tests were carried out after 56 days of curing in moist storage. For models with the bond between concretes, half of the specimens were made with substrate materials (C25, C45, and C60). After 21 days of curing the substrate in moist storage,

the models were removed for air curing at room temperature for six days. Subsequently, the surface treatment was carried out with a steel brush, and the wetting conditions were applied according to Table 3. After 24 h of wetting conditions, the remaining half of the specimen was overlaid with repair materials (C25, C45, C60, or UHPC). Specimens were molded for the mechanical test of the UHPC, curing in moist storage for 28 days, still at this stage. After 56 days of curing the substrate material and 28 days of repair, bond investigation tests were carried out.

**Table 3.** Studied parameters used in the tests.

Parameter	Detailed Situation
Treatment of substrate surface	Wire brushed
Moisture degree of substrate	Air surface dry (ASD) and saturated surface dry conditions (SSD)
Strength of substrate	Class-60, Class-45 and Class-25
Strength of repair	Class-60, Class-45, Class-25 and UHPC

### 2.2.3. Studied Parameters

Table 3 presents the parameters that affected the mechanical behavior of the bond between concretes, as evaluated in this study. The wetting conditions considered were the air-dry substrate with a dry surface (ASD) and the saturated substrate with a dry surface (SSD). For the ASD condition, specimens were removed from moist storage seven days before testing and kept at room temperature ( $25 \pm 2$  °C). Similarly, for the SSD condition, specimens were removed seven days before casting, submerged in water for the last 24 h before testing, and superficially dried with a cotton towel. The substrate surface treatment parameter was wire brushing, and the substrate was brushed in the bond region in all samples using an electric drill and a stainless-steel wire wheel brush. This treatment was carried out seven days before casting the repairs, in both vertical and horizontal directions for approximately 2 min, to remove undesirable impurities without exposing the aggregates, as shown in Figure 2. This procedure was similarly performed in studies by Carbonell Muñoz et al. [4,38], who concluded that a simple treatment that removes dust and debris from the substrate might be sufficient to obtain an excellent NSC–UHPC bond, provided that the substrate has an SSD condition.

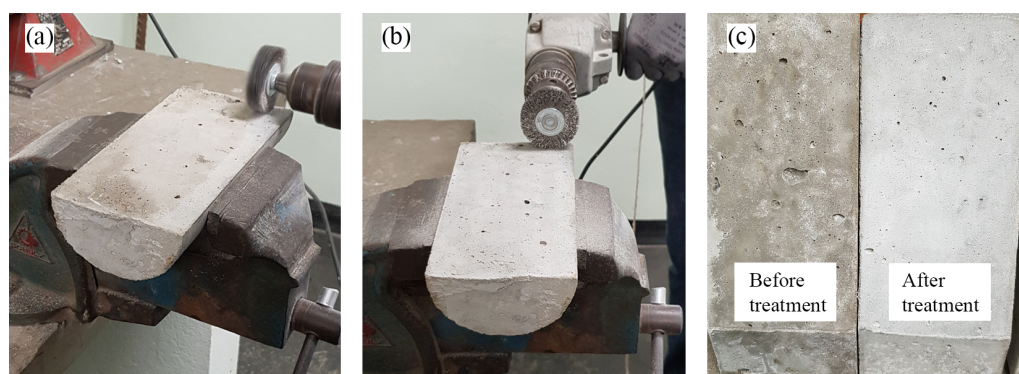


**Figure 2.** Surface treatment of composite models: (a) wire brushing in the vertical position; (b) wire brushing in the horizontal direction; (c) comparison of surfaces.

## 3. Results Analysis

### 3.1. Properties of Concretes

The slump values were within the range of  $80 \pm 20$  mm for C25 and C45 concrete. The C60 presented a 150 mm slump due to using a polycarboxylate water reducer. The UHPC spread test result was 450 mm, lower than that observed in the literature [40], whereas the average spread for UHPC is between 550 and 750 mm. However, it was possible to mold the UHPC in the specimens without requiring manual compacting or vibration.

The results of the concrete mechanical properties are presented in Table 4.

**Table 4.** Mechanical characteristics of concretes and UHPC.

Material	$f_c$ (MPa)	$sd$ (MPa)	$Cov$ (%)	$f_{sp}$ (MPa)	$sd$ (MPa)	$Cov$ (%)	$E_c$ (GPa)	$sd$ (GPa)	$Cov$ (%)
C25	26.05	0.99	3.81	2.78	0.01	0.29	29.90	1.19	3.98
C45	46.62	2.81	6.04	3.83	0.10	2.73	32.87	1.35	4.10
C60	59.65	2.81	4.70	4.60	0.09	1.92	34.95	1.37	3.93
UHPC	120.18	10.98	9.14	9.42	1.43	15.21	44.56	2.27	5.10

Nomenclature:  $f_c$  is the compressive strength of concrete;  $f_{sp}$  is the splitting tensile strength of concrete;  $E_c$  is the modulus of elasticity of concrete;  $sd$  is the standard deviation;  $Cov$  is the coefficient of variation.

For the splitting tensile test, the values found were close to the average theoretical tensile strength of concrete  $f_{ctm}$ , provided by fib MC 2010 [41] and EC 2 [42], with a difference of less than 10%. Similarly, the results of the modulus of elasticity of the concrete were compared with the theoretical  $E_c$ , provided by fib MC 2010 [41] and EC 2 [42], and with a recent equation proposed by Vakhshouri and Nejadi [43], and presented similar values.

For UHPC, the axial compressive strength results presented values above 120 MPa, without the addition of steel fibers in the mixture, classifying the material as ultra-high performance [44,45]. As for the splitting tensile test, the result is within the range observed in the literature [46], i.e., between 8 and 12 MPa. Finally, for the modulus of elasticity, values close to those found in the literature were found [40,44,47,48], and the average value of the UHPC elastic modulus was 45 GPa.

### 3.2. Model Classification

Commonly used as parameters in research, the ACI 546.3R-14 guide [20] and the study by Sprinkel and Ozyildirim [21] present the minimum requirements and classification of the bond between concretes based on their strengths submitted to different loads. The values are presented in Tables 5 and 6.

**Table 5.** Minimum acceptable slant shear and direct tensile bond strengths according to ACI 546.3R-14 [20].

Description	Bond Strength (MPa)		
	At 1st Day	At 7th Day	At 28th Day
Slant shear	2.8–6.9	6.9–12	14–21
Direct tensile	0.5–1	1.0–1.7	1.7–2.1

**Table 6.** Quantitative bond quality in terms of the tensile bond strength according to Sprinkel and Ozyildirim [21].

Bond Quality	Bond Strength (MPa)
Excellent	$\geq 2.1$
Very good	1.7–2.1
Good	1.4–1.7
Fair	0.7–1.4
Poor	0–0.7

### 3.3. Failure Modes

When carrying out the tests, the failure modes were identified according to Figure 3, as (a) failure mode A: adhesive failure, causing separation between the materials in the interface region; (b) failure mode B: mixed failure, with separation occurring at the interface with substrate detachment; (c) FAILURE mode C: cohesive failure, with the substrate failure.

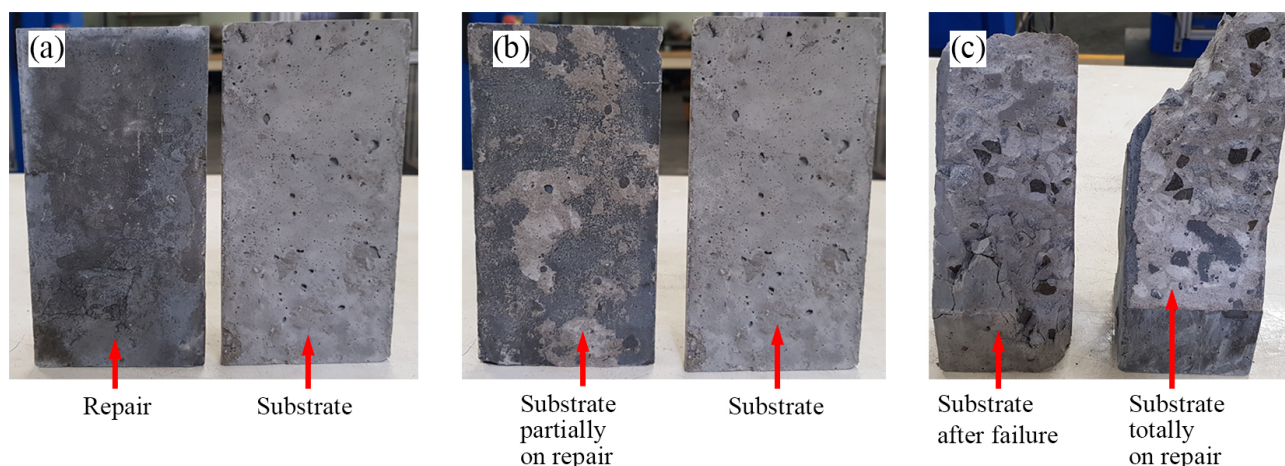


**Figure 3.** Typical failure modes: (a) failure mode A: adhesive failure; (b) failure mode B: mixed failure; (c) failure mode C: cohesive failure.

### 3.4. Test Results

The results of the slant shear and splitting tensile tests are presented in Table 7, including individual and average values ( $f_n$ ,  $\sigma_n$ ,  $\tau_n$ , and  $f_{sp}$ ), the coefficient of variation ( $Cov$ ), the typical rupture mode, and classification according to the literature [20,21] for each evaluated group. Where  $f_n$ ,  $\sigma_n$ ,  $\tau_n$ , and  $f_{sp}$  are calculated according to Equations (1) and (2) from the test results.

According to the test results, the bond can be classified by the ACI 546.3R-14 guide [20] and Sprinkel and Ozyildirim [21]. In the slant shear test, the models classified as sufficient, according to the minimum requirements of the ACI 546-3R-14 guide [20], were SSD-C45-UHPC and SSD-C60-UHPC. In the splitting tensile test, the only model studied that was classified as sufficient by the ACI 546-3R-14 guide [20] was the SSD-C60-UHPC. In the classification of Sprinkel and Ozyildirim [21], the only model rated as “Excellent” was the SSD-C60-UHPC. Other models such as SSD-C25-UHPC, SSD-C45-UHPC, ASD-C60-UHPC, and SSD-C60-C60 were rated “Very good”, confirming the contribution of HSC or UHPC as a repair material in wet conditions.

The result behaviors found can be observed in Figure 4. In the slant shear test, an increase in bond strength was observed in all groups with UHPC repair, regardless of whether the wetting conditions of the ASD or SSD substrate were used. This behavior was also observed in other studies [7,27]. Except for the ASD-C60-UHPC model, when UHPC was used as a repair material, failure mode B was observed in some specimens, with partial failure occurring in the lower concrete strength of the bond. Failure mode C was observed only in the SSD-C45-UHPC model, which could explain the occurrence of local defects in the substrate concrete. This behavior is consistent with the splitting tensile test results observed in other studies [27,37]. In all SSD models using UHPC as the repair material, failure mode B was observed in some specimens, with partial failure occurring in the substrate. The UHPC overlay generally contributes to the bond due to its high compressive strength and strong adhesion to the substrate concrete. Furthermore, the coefficient of variation ( $Cov$ ) of the NSC-UHPC bond strength in all experiments ranged from 6.61% to 9.29%, similar to values obtained by other studies [4,22,27].

Table 7. Experimental results in the slant shear and splitting tensile tests.

Identification	Slant Shear Test										Splitting Tensile Test						Classification of Bond	
	Sample 1 (kN)	Sample 2 (kN)	Sample 3 (kN)	Sample 4 (kN)	$f_n$ (MPa)	$\sigma_n$ (MPa)	$\tau_n$ (MPa)	Cov (%)	Failure Mode	Sample 1 (kN)	Sample 2 (kN)	Sample 3 (kN)	Sample 4 (kN)	$f_{sp}$ (MPa)	Cov (%)	Failure Mode	ACI [20]	Sprinkel and Ozyildirim [21]
C25	243.33	249.54	252.45	240.25	12.32	6.16	10.67	2.27	–	68.38	69.48	68.61	68.81	7.75	0.69	–	–	–
ASD-C25-C25	95.97	97.69	90.35	99.76	4.80	2.40	4.15	4.21	A	27.90	31.25	26.11	28.15	0.89	7.53	A	Insuf./Insuf.	Fair
ASD-C25-UHPC	144.02	135.86	159.12	137.98	7.21	3.61	6.25	7.28	A/B	46.93	39.96	39.60	44.08	1.49	8.22	A/B	Insuf./Insuf.	Fair
SSD-C25-C25	107.60	99.18	111.71	105.90	5.30	2.65	4.59	4.92	A	32.16	35.13	35.45	36.30	1.02	5.18	A	Insuf./Insuf.	Fair
SSD-C25-UHPC	230.19	218.78	206.32	250.55	11.32	5.66	9.81	8.30	A/B	58.79	50.58	62.47	57.22	1.87	8.68	A/B	Insuf./Suf.	Very good
C45	289.23	307.25	294.93	298.75	14.88	7.44	12.88	2.54	–	92.63	90.50	88.69	99.04	2.95	4.87	–	–	–
ASD-C45-C45	123.23	121.11	112.83	131.36	6.11	3.05	5.29	6.23	A	39.89	36.99	34.09	33.64	1.27	8.02	A	Insuf./Insuf.	Fair
ASD-C45-UHPC	172.60	187.33	159.94	173.46	8.67	4.33	7.51	6.46	A	49.33	45.53	51.79	43.57	1.57	7.78	A/B	Insuf./Insuf.	Good
SSD-C45-C45	151.23	139.52	140.85	128.91	7.01	3.50	6.07	6.51	A	46.97	49.31	41.30	43.53	1.50	7.86	A	Insuf./Insuf.	Good
SSD-C45-UHPC	311.09	276.21	290.77	261.05	14.24	7.12	12.33	7.49	A/B/C	70.67	60.40	61.92	67.10	2.25	7.28	A/B	Suf./Suf.	Very good
C60	432.45	454.23	415.63	433.99	21.70	10.85	18.80	3.64	–	141.00	131.14	137.62	125.88	4.49	5.03	–	–	–
ASD-C60-C60	162.35	168.38	173.83	187.76	8.65	4.33	7.49	6.27	A	44.94	48.26	42.21	39.40	1.43	8.67	A	Insuf./Insuf.	Good
ASD-C60-UHPC	210.37	225.33	195.37	198.04	10.36	5.18	8.98	6.61	A	61.31	50.52	56.73	51.10	1.95	9.29	A	Insuf./Insuf.	Very good
SSD-C60-C60	266.43	229.98	224.40	257.17	12.22	6.11	10.59	8.37	A	57.82	61.02	53.67	57.49	1.84	5.23	A	Insuf./Insuf.	Very good
SSD-C60-UHPC	347.28	379.04	328.66	309.87	17.06	8.53	14.77	8.64	B	80.23	95.31	83.71	85.14	2.55	7.52	A/B	Suf./Suf.	Excellent

Note: A, B, and C represent the typical failure modes shown in Figure 3; Insuf.: Insufficient; Suf.: Sufficient.

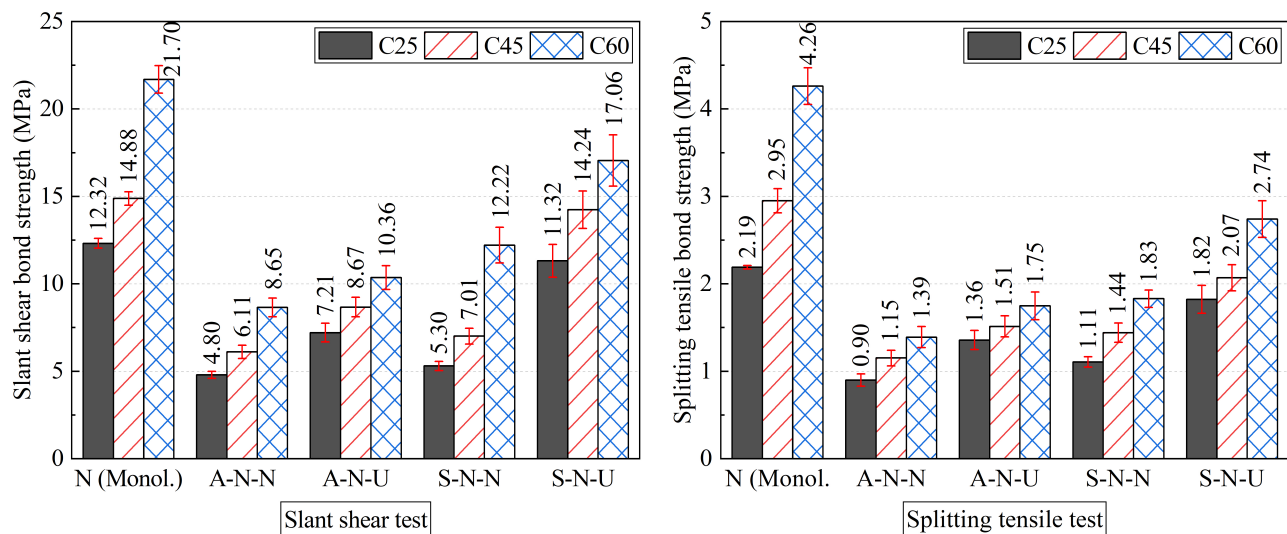


**Figure 4.** Experimental results of slant shear and splitting tensile tests. Nomenclature: A is the ASD wetting condition; S is the SSD wetting condition; N is the NSC or HSC concrete; U is the UHPC.

#### 4. Effects of Studied Parameters

##### 4.1. Moisture Degree of Substrate

To evaluate the influence of substrate-wetting conditions on the bond strength between concretes within each group, the values obtained in the tests for ASD conditions were compared to those obtained for the SSD models. This relationship is shown in Figure 5.

It can be seen in both tests that when changing the substrate-wetting conditions from SSD to ASD, the bond strength decreases in all models, regardless of the repair material. This behavior was also observed in other studies [4,26,27,49] and explained by the high porosity of the substrate concrete, which can transfer water through the interface, reducing the water available for repair material and generating incomplete cement hydration, thereby weakening the bond. However, wetting conditions have a more significant impact when using high-strength concretes as repair materials. In the case of HSC and UHPC, as they have a lower w/c ratio than NSC, if the substrate absorbs part of the water from these materials, the remaining amount is not sufficient for complete hydration of the cement, leading to a decrease in performance and weakening of the bond. The most significant reduction in bond strength under ASD substrate conditions occurred when using UHPC as a repair material, with reductions of around 40%, 40%, and 36% in the slant shear test and 36%, 27%, and 25% in the splitting tensile test for substrates C60, C45, and C25, respectively. The most considerable decreases were observed in models with UHPC, C60, C45, and C25 repair concrete. When using normal-strength concrete as a repair material, as it has a higher w/c ratio, the wetting conditions have a lesser influence on the bond strength because the water absorbed by the substrate will not be enough to compromise the cement hydration reaction of the overlay. This observation is reflected in the results of the slant shear test, where the ASD-C25-C25 model showed a decrease of only 10% compared to the SSD-C25-C25 model.

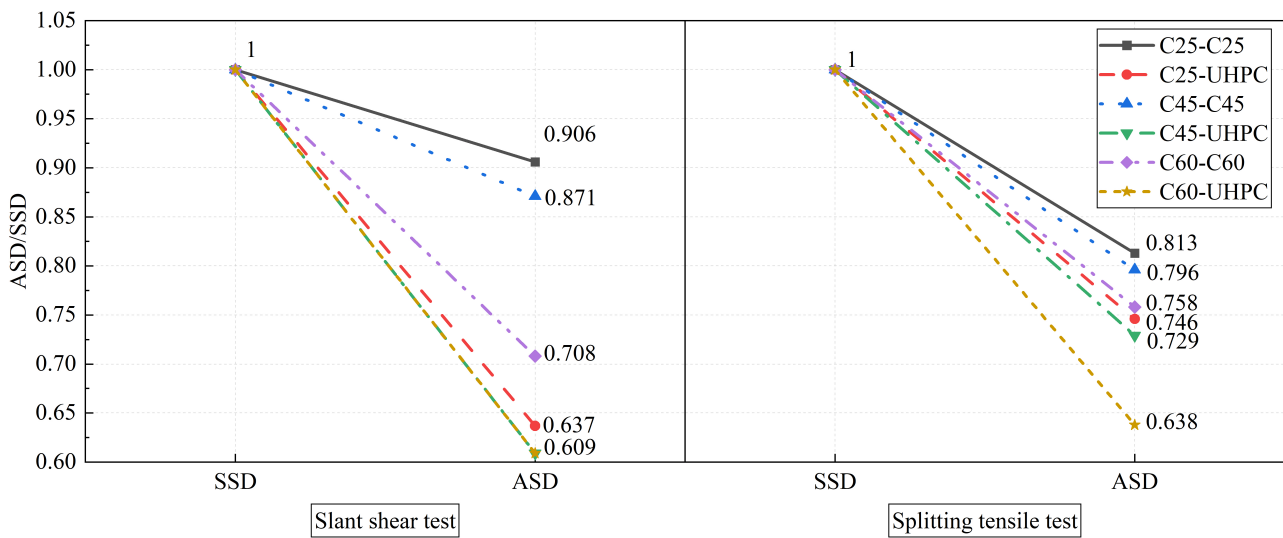


Figure 5. Effects of different moisture degrees of the substrate on the interfacial bond strength.

#### 4.2. Strength of Substrate

To evaluate the influence of substrate strength on the bond between concretes, specimens with C45 and C25 were compared to the results obtained with C60, with UHPC fixed as the repair. This relationship is shown in Figure 6.

Both test results show that regardless of the wetting conditions when changing the substrate to C45 and C25, the bond strength decreases compared to the C60 models. This behavior occurred because C60 has more tensile strength than C45 and C25 concretes. In the splitting tensile test, the bond strength of the SSD-C45-UHPC model was proportional to the decrease in the substrate strength by 25%. In the other models, the reduction in bond strength was not proportional to the decrease in the strength of the substrate concrete.

The bond strength decrease is more significant in substrates with lower strength concretes and SSD wetting conditions compared to the ASD group; this is due to the strength of the ASD-C60-UHPC model being lower than that of the SSD-C60-UHPC, at around 39% and 36% for slant shear and splitting tensile tests, respectively.

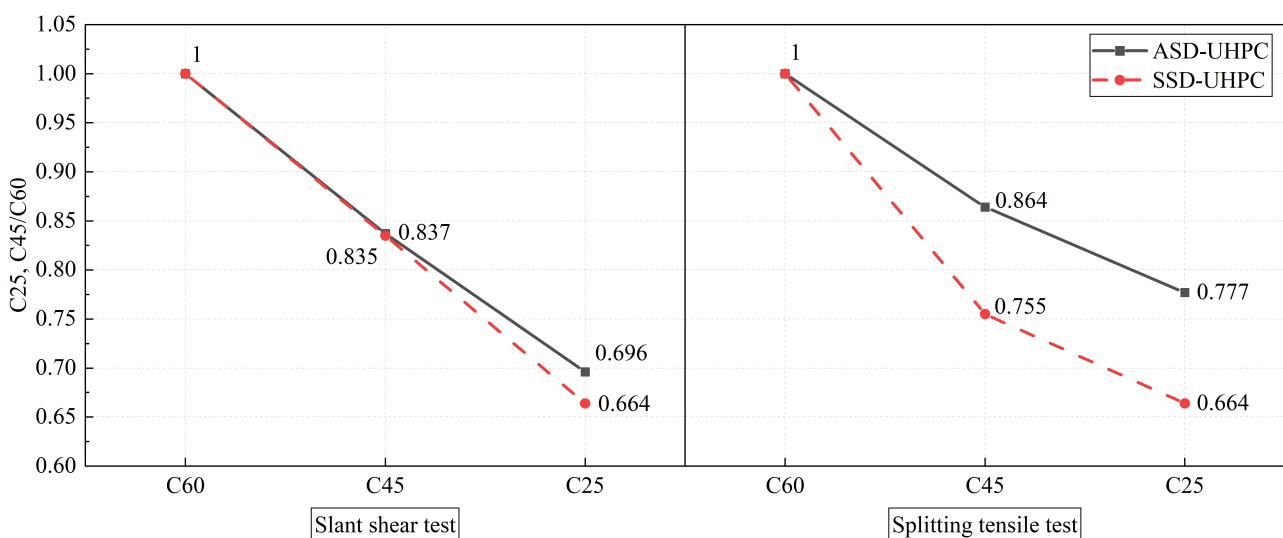


Figure 6. Effects of the substrate strength on the interfacial bond strength.

### 4.3. Strength of Repair

In order to evaluate the influence of the repair strength on the bond between concretes, the test results were compared to monolithic specimens. This allows for verification of the contribution of the repair material change within each group and comparison to monolithic strength. This relationship is shown in Figure 7.

The mechanism of the bond between concretes is influenced by cohesion, due to adherence, friction, or the roughness of the substrate surface. It is evident from the results of the splitting tensile test that stronger concrete repairs provide better adherence to the bond. However, in the results of the slant shear test, the contribution of strength of the concrete repair to the models with C45 and C60 substrates was not adequately evidenced. This behavior can be explained by the fact that the surface treatment of the substrate adopted was not sufficient to provide adequate roughness.

All of the SSD models exhibited higher bond strengths compared to the ASD models. The most significant strength increase was observed in SSD models with lower strength substrates, with UHPC as the repair material, where the adhesion was so strong that several specimens showed failure modes B and C. The SSD-C25-UHPC model was particularly noteworthy, demonstrating around 92% and 83% of the respective monolithic model strength in the slant shear and splitting tensile tests, respectively. Similarly, the SSD-C45-UHPC model demonstrated around 96% and 70% of the respective monolithic model strength in the slant shear and splitting tensile tests, respectively. Therefore, the hypothesis that the most significant bond strength reductions occur in ASD models with HSC or UHPC as the repair material was confirmed. The ASD-C60-UHPC model exhibited around 48% and 41%, of the strength of its respective monolithic model in the slant shear and splitting tensile tests, respectively, while the ASD-C60-C60 model exhibited around 40% and 33% of the strength of its respective monolithic model in the slant shear and splitting tensile tests, respectively.

When C25 and C45 were used as repair materials, the strength decreased, regardless of the substrate's wetting conditions, confirming the low influence of this parameter in lower repair concrete strength. For these models, the bond strength was 39% and 47% in the slant shear tests and 32% and 49% in the splitting tensile tests, compared to monolithic models.

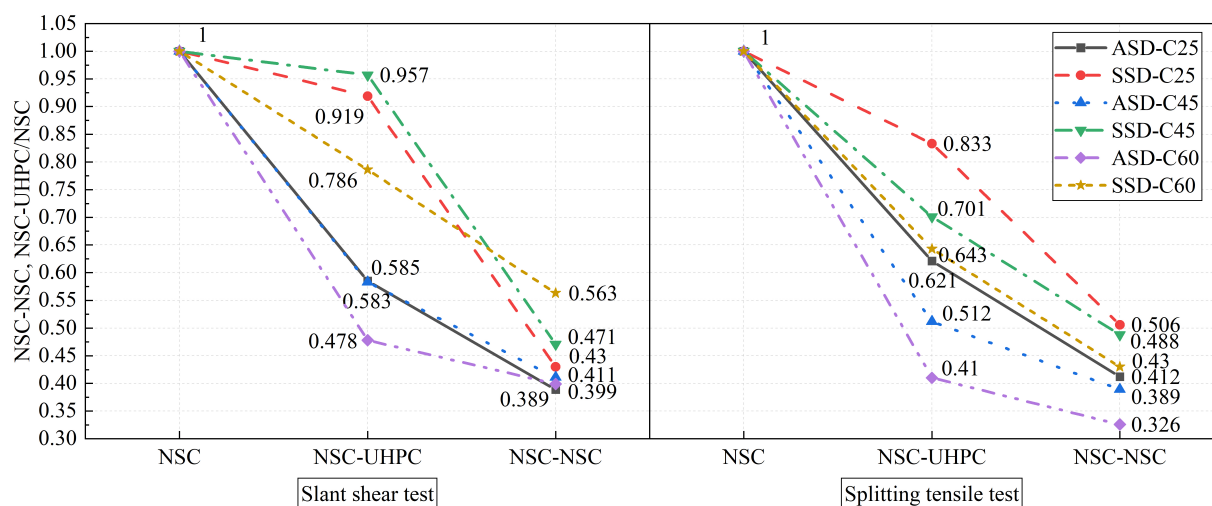


Figure 7. Effects of the repair strength on the interfacial bond strength.

### 5. Cohesion and Friction Coefficient

Based on the Mohr–Coulomb theory, international standards, and research, some models have been developed for predicting the shear capacity of the bond between cementitious composites and specifying design values for cohesion and friction coefficients, as presented in Table 8.

**Table 8.** Models for predicting bond strength between concretes.

Sources	Model	Values Adopted for Wire Brushed Substrate	
		Cohesion	Coefficient of Friction $\mu$
fib MC 2010 [41]	$\tau_u = c_a f_{ctd} + \mu \sigma_n$	0.40	0.70–1.00
EC 2 [42]	$\tau_u = c_a f_{ctd} + \mu \sigma_n$	0.40	0.70
CSA S6-14 [50]	$\tau_u = \phi_c \left[ c + \mu \left( \frac{P_c}{A_{cv}} \right) \right]$	0.50	1.00
AASHTO LRFD [29]	$V_n = c A_{cv} + \mu P_c$	1.65	1.00
Santos and Júlio [30,51]	$\tau_u = c_a f_{ctd} + \mu \sigma_n$	$c_a = \frac{1.062 R_{vm}^{0.145}}{\gamma_{coh}}$	$\mu = \frac{1.366 R_{vm}^{0.041}}{\gamma_{fr}}$
Mohamad et al. [52]	$\tau_u = c_a f_{ctd} + \mu \sigma_n$	$c_a = 0.2363 e^{0.237 R_{pm}}$	$\mu = 0.8766 R_{pm}^{0.3978}$

Nomenclature:  $\tau_u$  is the shear strength of the interface;  $\sigma_n$  is the normal voltage acting on the interface;  $c_a$  is the coefficient for adhesive bonding;  $\mu$  is the coefficient of friction;  $f_{ctd}$  is the design tensile strength of the concrete;  $\phi_c$  is the concrete strength reduction factor (recommended value of 0.75 by the standard);  $P_c$  is the normal force acting on the shear interface, if the force acting on the interface is tensile, then  $P_c = 0$ ;  $V_n$  is the maximum shear force acting on the shear interface;  $R_{vm}$  is a roughness parameter that represents the maximum depth of the valley (for wire brushed it is equivalent to 0.473);  $\gamma_{coh}$  is a partial safety factor of the cohesion coefficient (recommended by the authors a value of 2.60);  $\gamma_{fr}$  is a partial safety factor for the coefficient of friction (the authors recommend a value of 1.20);  $R_{pm}$  is a roughness parameter that represents the average height of the crest (for wire brushed between 4.47 and 7.67).

In the present study, cohesion values were used as the results of splitting tensile tests ( $f_{sp}$ ). With the cohesion values and the results of the slant shear test, it is possible to find the value of the friction coefficient and, consequently, the friction angle. Table 9 compares experimental and analytical results.

**Table 9.** Predictive values of the bond strength between concretes.

Sources	Identification	Slant Shear Test		Splitting Tensile Test	Coefficient of Friction $\mu$	Friction Angle $\phi$ (°)
		$\sigma_n$ (MPa)	$\tau_n$ (MPa)	$f_{sp}$ or $c$ (MPa)		
This study	C25	6.16	10.67	2.19	1.38	54.02
	ASD-C25-C25	2.40	4.16	0.90	1.36	53.61
	ASD-C25-UHPC	3.61	6.25	1.36	1.36	53.58
	SSD-C25-C25	2.65	4.59	1.11	1.31	52.73
	SSD-C25-UHPC	5.66	9.81	1.82	1.41	54.67
	C45	7.44	12.89	2.95	1.34	53.17
	ASD-C45-C45	3.05	5.29	1.15	1.36	53.60
	ASD-C45-UHPC	4.34	7.51	1.51	1.38	54.15
	SSD-C45-C45	3.50	6.07	1.44	1.32	52.88
	SSD-C45-UHPC	7.12	12.33	2.07	1.44	55.25
	C60	10.85	18.79	4.26	1.34	53.26
	ASD-C60-C60	4.33	7.49	1.39	1.41	54.68
	ASD-C60-UHPC	5.18	8.98	1.75	1.39	54.36
	SSD-C60-C60	6.11	10.58	1.83	1.43	55.08
	SSD-C60-UHPC	8.53	14.77	2.74	1.41	54.67
	MC2010 [41], EC2 [42] <sup>(1)</sup>	C25	–	–	0.48	0.70
C45		–	–	0.71	0.70	34.99
C60		–	–	0.81	0.70	34.99
MC2010 [41], EC2 [42] <sup>(2)</sup>	C25	–	–	1.23	0.70	34.99
	C45	–	–	1.53	0.70	34.99
	C60	–	–	1.84	0.70	34.99
CSA S6-14 [50]	Mixed	–	–	0.50	1.00	45.00
	Mixed	–	–	1.65	1.00	45.00
AASHTO LRFD [29]	C25	–	–	0.44	1.10	47.73
	C45	–	–	0.65	1.10	47.73
	C60	–	–	0.74	1.10	47.73
Santos and Júlio [30,51] <sup>(1)</sup>	C25	–	–	1.16	1.10	47.73
	C45	–	–	1.40	1.10	47.73
	C60	–	–	1.69	1.10	47.73
Santos and Júlio [30,51] <sup>(2)</sup>	C25	–	–	0.82	1.59	57.84
	C45	–	–	1.21	1.59	57.84
	C60	–	–	1.39	1.59	57.84
Mohamad et al. [52] <sup>(1)</sup>	C25	–	–	1.89	1.59	57.84
	C45	–	–	2.61	1.59	57.84
	C60	–	–	3.14	1.59	57.84
Mohamad et al. [52] <sup>(2)</sup>	C25	–	–	–	–	–
	C45	–	–	–	–	–
	C60	–	–	–	–	–

Note: <sup>(1)</sup>: results from the  $f_{ctd}$  theoretical, calculated according to MC 2010 standards [41] e EC 2 [42]; <sup>(2)</sup>: results substituting  $f_{ctd}$  for the average of the tensile strength of the lower strength concrete of the bond, obtained in experimental tests in the present study.

The AASHTO LRFD coefficients [29] apply to the SSD-C25-UHPC, SSD-C45-UHPC, ASD-C60-UHPC, SSD-C60-C60, and SSD-C60-UHPC models. When using the theoretical values of  $f_{ctd}$  calculated by standards, the fib MC 2010 [41], EC 2 [42], and Santos and Júlio [30,51] methods provide a safety margin for all models studied. The prediction model proposed by Mohamad et al. [52] provides a safety margin for all models with UHPC repair

and the SSD-C60-C60. When replacing  $f_{ctd}$  with experimental values of concrete tensile strength, the fib MC 2010 [41], EC 2 [42], and Santos and Júlio [30,51] methods provide a safety margin for all models with UHPC repair. The method by Mohamad et al. [52] does not describe any model, as the values above the results were found experimentally.

For models with substrate C25 and C45, the most conservative methods were proposed by fib MC 2010 [41] and EC 2 [42]. The most conservative methods were proposed in models with C60 substrates by CSA S6-14 [50]. Therefore, no prediction models in the literature considered some of the parameters, such as the wetting conditions and the repair concrete strength, which needed more investigation.

For the structural repair or rehabilitation design, the correct specifications of wetting conditions and roughness of concrete substrates are recommended. As for the structure's response, the bond between the concrete should not present brittle rupture. Thus, the cohesion and the coefficient of friction must present high values so that the substrate fails before the bond.

## 6. Conclusions

From investigating the bond between concretes with different substrate surface wetting conditions, substrate concrete strength, and repair concrete strength, the following conclusions can be drawn:

1. Regarding the standard minimum requirements of the bond between concretes, the only model classified as "Sufficient" was the SSD-C60-UHPC. According to other research, several others were classified as "Excellent" or "Very good";
2. The results showed that when changing the substrate-wetting conditions from SSD to ASD, the bond strength decreases in all models studied, which can be explained by the high porosity of the substrate concrete can transfer water through the interface, which reduces the water in the repair material, which generates incomplete cement hydration, weakening the bond. The most expressive strength gains occur in SSD models with lower substrate strengths and UHPC as a repair material. Likewise, it was confirmed that the most significant reductions occur in ASD models with higher substrate strengths and HSC or UHPC as repair material;
3. When lower-strength concrete was used as the repair material, the substrate-wetting conditions had a minor influence on the bond strength;
4. From the present study, wet substrate conditions should be used whenever HSC or UHPC is used as the repair material for aged concrete structures;
5. When analyzing the bond strength predicting models between concretes, the AASHTO LRFD standard [29] is valid only for models with SSD and UHPC substrates as repair materials. The most conservative method was proposed by fib MC 2010 [41] and EC 2 [42], where the cohesion and friction coefficient results were, on average, 49% and 35% less than the models studied, respectively. The least conservative, however, was the method proposed by Mohamad et al. [52], where the results of the cohesion and friction coefficient were, on average, 15% and 7% higher than the models studied, respectively;
6. In order to better describe the models with repairs in UHPC, it was suggested by the fib MC 2010 [41], EC 2 [42], and Santos and Júlio [30,51] methods to substitute the variable  $f_{ctd}$  by the average of the substrate tensile strength obtained experimentally, or by  $f_{ctm}$ , without a safety factor. Unlike the method by Mohamad et al. [52], using  $f_{ctm}$  does not represent any of the models studied. However, substituting  $f_{ctm}$  with  $f_{ctd}$ , the method is the one that better represents the NSC-UHPC models studied.

The present paper limits the study of some parameters that influence the bond between concretes, such as wetting surface conditions and the strength of both substrate and repair materials. However, other parameters need more investigation and can be applied in future research, such as the effects of elevated temperatures on the bond between concretes and the development of innovative and practicable HSC surface treatment to guarantee an adequate structural response.

**Author Contributions:** V.B.d.S.: Conceptualization, Formal analysis, Investigation, Methodology, Validation, Writing—original draft, Writing—review and editing. A.P.P.d.S.S.: Investigation, Validation, Visualization, Writing—review and editing. B.L.P.: Visualization, Writing—review and editing. L.D.T.: Visualization, Writing—review and editing. P.A.K.: Formal analysis, Visualization, Writing—review and editing. R.D.V.: Methodology, Supervision, Writing—review and editing. All authors have read and agreed to the published version of the manuscript.

**Funding:** This research received no external funding.

**Data Availability Statement:** Data available on request from the authors.

**Acknowledgments:** This study was financed in part by the Coordenação de Aperfeiçoamento de Pessoal de Nível Superior-Brasil (CAPES)-Finance Code 001.

**Conflicts of Interest:** The authors declare no conflict of interest.

## References

- Brühwiler, E.; Denarié, E. Rehabilitation of concrete structures using Ultra-High Performance Fibre Reinforced Concrete. In Proceedings of the Second International Symposium on Ultra High Performance Concrete, Kassel, Germany, 5–7 March 2008; pp. 1–8.
- Brühwiler, E.; Denarié, E. Rehabilitation and Strengthening of Concrete Structures Using Ultra-High Performance Fibre Reinforced Concrete. *Struct. Eng. Int.* **2013**, *23*, 450–457. [[CrossRef](#)]
- Tayeh, B.A.; Abu Bakar, B.H.; Megat Johari, M.A.; Voo, Y.L. Evaluation of Bond Strength between Normal Concrete Substrate and Ultra High Performance Fiber Concrete as a Repair Material. *Procedia Eng.* **2013**, *54*, 554–563. [[CrossRef](#)]
- Carbonell Mu noz, M.A.; Harris, D.K.; Ahlborn, T.M.; Froster, D.C. Bond Performance between Ultrahigh-Performance Concrete and Normal-Strength Concrete. *J. Mater. Civ. Eng.* **2014**, *26*, 04014031. [[CrossRef](#)]
- Al-Osta, M.A.; Isa, M.N.; Baluch, M.H.; Rahman, M.K. Flexural behavior of reinforced concrete beams strengthened with ultra-high performance fiber reinforced concrete. *Constr. Build. Mater.* **2017**, *134*, 279–296. [[CrossRef](#)]
- Ramachandra Murthy, A.; Karihaloo, B.L.; Priya, D.S. Flexural behavior of RC beams retrofitted with ultra-high strength concrete. *Constr. Build. Mater.* **2018**, *175*, 815–824. [[CrossRef](#)]
- Farzad, M.; Shafieifar, M.; Azizinamini, A. Experimental and numerical study on bond strength between conventional concrete and Ultra High-Performance Concrete (UHPC). *Eng. Struct.* **2019**, *186*, 297–305. [[CrossRef](#)]
- Xie, J.; Fu, Q.; Yan, J.B. Compressive behaviour of stub concrete column strengthened with ultra-high performance concrete jacket. *Constr. Build. Mater.* **2019**, *204*, 643–658. [[CrossRef](#)]
- Zhu, Y.; Zhang, Y.; Hussein, H.H.; Chen, G. Flexural strengthening of reinforced concrete beams or slabs using ultra-high performance concrete (UHPC): A state of the art review. *Eng. Struct.* **2020**, *205*, 110035. [[CrossRef](#)]
- Tayeh, B.A.; Abu Bakar, B.H.; Megat Johari, M.A. Characterization of the interfacial bond between old concrete substrate and ultra high performance fiber concrete repair composite. *Mater. Struct.* **2013**, *46*, 743–753. [[CrossRef](#)]
- Aziz, Y.H.A.; Zaher, Y.A.; Wahab, M.A.; Khalaf, M. Predicting temperature rise in Jacketed concrete beams subjected to elevated temperatures. *Constr. Build. Mater.* **2019**, *227*, 116460. [[CrossRef](#)]
- El-Khier, M.A.; Morcous, G. Precast concrete deck-to-girder connection using Ultra-High Performance Concrete (UHPC) shear pockets. *Eng. Struct.* **2021**, *248*, 113082. [[CrossRef](#)]
- Fang, Z.; Fang, H.; Li, P.; Jiang, H.; Chen, G. Interfacial shear and flexural performances of steel–precast UHPC composite beams: Full-depth slabs with studs vs. demountable slabs with bolts. *Eng. Struct.* **2022**, *260*, 114230. [[CrossRef](#)]
- Júlio, E.N.B.S.; Dias-da Costa, D.; Branco, F.A.B.; Alfaiate, J.M.V. Accuracy of design code expressions for estimating longitudinal shear strength of strengthening concrete overlays. *Eng. Struct.* **2010**, *32*, 2387–2393. [[CrossRef](#)]
- Espeche, A.D.; León, J. Estimation of bond strength envelopes for old-to-new concrete interfaces based on a cylinder splitting test. *Constr. Build. Mater.* **2011**, *25*, 1222–1235. [[CrossRef](#)]
- Sanchez-Silva, M.; Klutke, G.A.; Rosowsky, D.V. Life-cycle performance of structures subject to multiple deterioration mechanisms. *Struct. Saf.* **2011**, *33*, 206–217. [[CrossRef](#)]
- AlHallaq, A.F.; Tayeh, B.A.; Shihada, S. Investigation of the Bond Strength between Existing Concrete Substrate and UHPC as a Repair Material. *Int. J. Eng. Adv. Technol. (IJEAT)* **2017**, *6*, 8.
- Rahman, A.; Ai, C.; Xin, C.; Gao, X.; Lu, Y. State-of-the-art review of interface bond testing devices for pavement layers: Toward the standardization procedure. *J. Adhes. Sci. Technol.* **2017**, *31*, 109–126. [[CrossRef](#)]
- Harris, D.K.; Sarkar, J.; Ahlborn, T.M. Characterization of Interface Bond of Ultra-High-Performance Concrete Bridge Deck Overlays. *Transp. Res. Rec. J. Transp. Res. Board* **2011**, *2240*, 40–49. [[CrossRef](#)]
- ACI. *ACI 546.3R-14: Guide to Materials Selection for Concrete Repair*; ACI: Farmington Hills, MI, USA, 2014; p. 72.
- Sprinkel, M.M.; Ozyildirim, C. *Evaluation of High Performance Concrete Overlays Placed on Route 60 over Lynhaven Inlet in Virginia (Report No. FHWA/VTRC 01-R1)*; Technical Report; Virginia Transportation Research Council: Charlottesville, VA, USA, 2000.
- Tayeh, B.A.; Abu Bakar, B.H.; Megat Johari, M.A.; Voo, Y.L. Mechanical and permeability properties of the interface between normal concrete substrate and ultra high performance fiber concrete overlay. *Constr. Build. Mater.* **2012**, *36*, 538–548. [[CrossRef](#)]

23. Youm, H.S.; Lim, W.Y.; Hong, S.G.; Joh, C.B. Evaluation of interfacial performance of normal strength concrete strengthened with ultra-high performance fiber reinforced concrete through slant shear test. *J. Korea Concr. Inst.* **2018**, *30*, 391–401. [[CrossRef](#)]
24. Abo Sabah, S.H.; Hassan, M.H.; Muhamad Bunnori, N.; Megat Johari, M.A. Bond strength of the interface between normal concrete substrate and GUSMRC repair material overlay. *Constr. Build. Mater.* **2019**, *216*, 261–271. [[CrossRef](#)]
25. Valikhani, A.; Jaber, A.; Mantawy, I.M.; Azizinamini, A. Experimental evaluation of concrete-to-UHPC bond strength with correlation to surface roughness for repair application. *Constr. Build. Mater.* **2020**, *238*, 117753. [[CrossRef](#)]
26. Zhang, Y.; Zhu, P.; Wang, X.; Wu, J. Shear properties of the interface between ultra-high performance concrete and normal strength concrete. *Constr. Build. Mater.* **2020**, *248*, 118455. [[CrossRef](#)]
27. Zhang, Y.; Zhu, P.; Liao, Z.; Wang, L. Interfacial bond properties between normal strength concrete substrate and ultra-high performance concrete as a repair material. *Constr. Build. Mater.* **2020**, *235*, 117431. [[CrossRef](#)]
28. Zhang, Y.; Zhang, C.; Zhu, Y.; Cao, J.; Shao, X. An experimental study: Various influence factors affecting interfacial shear performance of UHPC-NSC. *Constr. Build. Mater.* **2020**, *236*, 117480. [[CrossRef](#)]
29. AASHTO. *AASHTO LRF Bridge Design Specifications*, 6th ed.; AASHTO: Washington, DC, USA, 2012; p. 1912.
30. Santos, P.M.D.; Júlio, E.N.B.S. Factors Affecting Bond between New and Old Concrete. *ACI Mater. J.* **2011**, *108*, 449–456. [[CrossRef](#)]
31. Hussein, H.H.; Walsh, K.K.; Sargand, S.M.; Steinberg, E.P. Interfacial Properties of Ultrahigh-Performance Concrete and High-Strength Concrete Bridge Connections. *J. Mater. Civ. Eng.* **2016**, *28*, 04015208. [[CrossRef](#)]
32. Zanotti, C.; Randl, N. Are concrete-concrete bond tests comparable? *Cem. Concr. Compos.* **2019**, *99*, 80–88. [[CrossRef](#)]
33. ABNT NBR 5739; Concreto-Ensaio de Compressão de Corpos de Prova Cilíndricos. ABNT: Rio de Janeiro, Brazil, 2018; p. 9.
34. C496/C496M-17; Standard Test Method for Splitting Tensile Strength of Cylindrical Concrete Specimens. ASTM International: West Conshohocken, PA, USA, 2017; p. 5. [[CrossRef](#)]
35. ABNT NBR 8522-1; Concreto Endurecido-Determinação dos módulos de Elasticidade e de Deformação-Parte 1: Módulos Estáticos à Compressão. ABNT: Rio de Janeiro, Brazil, 2021; p. 20.
36. C882/C882M-13a; Standard Test Method for Bond Strength of Epoxy-Resin Systems Used with Concrete by Slant Shear. ASTM International: West Conshohocken, PA, USA, 2013; p. 4. [[CrossRef](#)]
37. Mansour, W.; Fayed, S. Effect of interfacial surface preparation technique on bond characteristics of both NSC-UHPFRC and NSC-NSC composites. *Structures* **2021**, *29*, 147–166. [[CrossRef](#)]
38. Carbonell Mu noz, M.A. Compatibility of Ultra High Performance Concrete as Repair Material: Bond Characterization with Concrete under Different Loading Scenarios. Master's Thesis, Michigan Technological University, Houghton, MI, USA, 2012.
39. C39/C39M-18; Compressive Strength of Cylindrical Concrete Specimens. ASTM International: West Conshohocken, PA, USA, 2018; p. 7. [[CrossRef](#)]
40. Akhnoorkh, A.K.; Buckhalter, C. Ultra-high-performance concrete: Constituents, mechanical properties, applications and current challenges. *Case Stud. Constr. Mater.* **2021**, *15*, e00559. [[CrossRef](#)]
41. Fib. *Fib Model Code for Concrete Structures 2010*; Wilhelm Ernst & Sohn: Berlin, Germany, 2013; p. 402.
42. EN 1992-1-1; Eurocode 2: Design of Concrete Structures—Part 1-1: General Rules and Rules for Buildings. CEN: Bruxelles, Belgium, 2004; p. 225.
43. Vakhshouri, B.; Nejadi, S. Empirical models and design codes in prediction of modulus of elasticity of concrete. *Front. Struct. Civ. Eng.* **2019**, *13*, 38–48. [[CrossRef](#)]
44. Graybeal, B.A. Compressive Behavior of Ultra-High-Performance Fiber-Reinforced Concrete. *ACI Mater. J.* **2007**, *104*, 146–152. [[CrossRef](#)]
45. Hassan, A.M.T.; Jones, S.W.; Mahmud, G.H. Experimental test methods to determine the uniaxial tensile and compressive behaviour of ultra high performance fibre reinforced concrete (UHPFRC). *Constr. Build. Mater.* **2012**, *37*, 874–882. [[CrossRef](#)]
46. Arora, A.; Almujaiddi, A.; Kianmofrad, F.; Mobasher, B.; Neithalath, N. Material design of economical ultra-high performance concrete (UHPC) and evaluation of their properties. *Cem. Concr. Compos.* **2019**, *104*, 103346. [[CrossRef](#)]
47. Habel, K.; Viviani, M.; Denarié, E.; Brühwiler, E. Development of the mechanical properties of an Ultra-High Performance Fiber Reinforced Concrete (UHPFRC). *Cem. Concr. Res.* **2006**, *36*, 1362–1370. [[CrossRef](#)]
48. Pourbaba, M.; Asefi, E.; Sadaghian, H.; Mirmiran, A. Effect of age on the compressive strength of ultra-high-performance fiber-reinforced concrete. *Constr. Build. Mater.* **2018**, *175*, 402–410. [[CrossRef](#)]
49. Semendary, A.A.; Svecova, D. Factors affecting bond between precast concrete and cast in place ultra high performance concrete (UHPC). *Eng. Struct.* **2020**, *216*, 110746. [[CrossRef](#)]
50. CSA. *S6-14: Canadian Highway Bridge Design Code*; CSA Group: Mississauga, ON, Canada, 2014; p. 875.
51. Santos, P.M.D.; Júlio, E.N.B.S. Recommended Improvements to Current Shear-Friction Provisions of Model Code. In Proceedings of the 3rd fib International Congress, Washington, DC, USA, 29 May–2 June 2010; p. 21.
52. Mohamad, M.E.; Ibrahim, I.S.; Abdullah, R.; Rahman, A.B.A.; Kueh, A.B.H.; Usman, J. Friction and cohesion coefficients of composite concrete-to-concrete bond. *Cem. Concr. Compos.* **2015**, *56*, 1–14. [[CrossRef](#)]

**Disclaimer/Publisher's Note:** The statements, opinions and data contained in all publications are solely those of the individual author(s) and contributor(s) and not of MDPI and/or the editor(s). MDPI and/or the editor(s) disclaim responsibility for any injury to people or property resulting from any ideas, methods, instructions or products referred to in the content.